Facile synthesis of silica nanoparticles grafted with quaternized linear, comblike and toothbrushlike copolymers

Journal:	*Polymer Chemistry*
Manuscript ID:	PY-ART-12-2014-001741.R1
Article Type:	Paper
Date Submitted by the Author:	26-Jan-2015
Complete List of Authors:	Zhao, Youliang; Soochow University, College of Chemistry, Chemical Engineering and Materials Science Guo, Yanfei; Soochow University, Liu, Huanhuan; Soochow University, Tang, Dandan; Soochow University, Li, Cangxia; Soochow University,

SCHOLARONE™
Manuscripts

Cite this: DOI: 10.1039/c0xx00000x

www.rsc.org/xxxxxx

ARTICLE TYPE

Facile synthesis of silica nanoparticles grafted with quaternized linear, comblike and toothbrushlike copolymers†

Yanfei Guo, Huanhuan Liu, Dandan Tang, Cangxia Li and Youliang Zhao*

Received (in XXX, XXX) Xth XXXXXXXXX 20XX, Accepted Xth XXXXXXXXX 20XX

DOI: 10.1039/b000000x

Facile construction of solid substrates grafted with quaternized copolymers by two step reactions comprising alkoxysilane-hydroxyl coupling reaction, quaternization and RAFT polymerization was described. Silica nanoparticles grafted with poly(*N,N*-dimethylaminoethyl methacrylate) (PDMA) was initially prepared via tandem linking reaction and RAFT polymerization and acted as a versatile platform to generate three types of ion-bearing topological copolymers grafted silica. Bromide-functionalized agents and polymers were grafted onto surface-tethered PDMA backbone to form quaternized random and comblike copolymers grafted silica, and concurrent quaternization and RAFT process were performed to generate silica nanoparticles grafted with toothbrushlike copolymers comprising poly(methyl methacrylate), polystyrene, poly(*N*-isopropylacrylamide) and poly(*tert*-butyl acrylate) segments. Free polymers and grafted side chains obtained by tandem approach usually had similar chain length and low polydispersity, evident from hydrolysis, GPC and ^{1}H NMR analyses. The quaternization efficiency of graft reactions was in the range 34-79% (for attaching small molecules) and 3.8-7.4% (for grafting polymeric chains). Our preliminary results revealed the surface wettability of hybrid films was dependent on some factors such as macromolecular architecture, quaternization degree, chemical composition and temperature. This study affords a straightforward and versatile method to construct quaternized macromolecular architectures grafted onto hydroxyl-rich solid substrates, and the resultant silica-polymer hybrids may have a great potential in stimuli-responsive emulsifiers, surface and antibacterial materials.

Surface modification of solid substrates with functional polymeric chains has attracted much attention due to their adjustable mechanical, surface and thermal properties and versatile applications in functional materials.[1–15] Among them, silica particles are substrates of choice to generate core-shell hybrid materials due to their many advantages such as chemical resistance, mechanical stability, variable particle sizes, and tunable specific surface area and pore size.[1–6] Based on reactive hydroxyl groups on silica surface, surface modifiers such as organoalkoxysilanes are easily linked to form surface-tethered functional groups, which further bridge inorganic and polymeric layers via postpolymerization modification. Surface-initiated controlled radical polymerization techniques involving reversible addition-fragmentation chain transfer (SI-RAFT) polymerization have been efficiently used to prepare silica-polymer hybrid materials, in which the graft reaction can be conducted via either "grafting to" or "grafting from" approach.[16–32] The former affords a straightforward route to give the target hybrids with relatively low grafting density due to steric hindrance, whilst the latter allows the formation of silica-polymer hybrids with higher grafting density although side reactions may lead to structural defects of grafted chains. SI-RAFT can be performed via either stepwise or tandem approach, however, the examples on tandem synthesis of polymers grafted solid substrates are very scarce thus far.[16,30–35] For example, Ranjan et al. utilized tandem RAFT polymerization and click chemistry to synthesize PSt grafted silica nanoparticles with a grafting density up to 0.51-0.70 chains nm^{-2},[16] and we have combined simultaneous RAFT process and linking reaction such as copper(I)-catalyzed azide-alkyne cycloaddition (CuAAC) reaction and alkoxysilane-hydroxyl coupling reaction to synthesize silica particles[30,31] and graphene oxide[32] grafted with a series of linear polymers up to tetrablock copolymers. As compared with traditional stepwise method, the tandem approach is more promising due to significant advantages in terms of labor, time and cost, and thus it is extremely important to further extend this method to prepare functional hybrids.

As one member of stimuli-responsive polymer family, poly(*N,N*-dimethylaminoethyl methacrylate) (PDMA) and its quaternized polymers have been widely investigated due to their pH and thermo-responsiveness.[36–67] PDMA acts as a weak polyelectrolyte with pH-tunable charge density due to the presence of ionizable tertiary amine moieties, and its lower critical solution temperature (LCST) is in the range 32-53 °C. As well documented, PDMA segments hydrate to swell and stretch in aqueous solution at a temperature below LCST, and they are liable to shrink and adopt a globular form at a temperature beyond LCST due to dehydration. These features endow PDMA-based copolymers grafted solid substrates with a wide range of potential applications such as nanoreactors,[48,49] carriers for drug and gene delivery,[50,51] separation membranes,[52–55] and

antibacterial materials. Furthermore, the quaternization modification of PDMA can introduce upper critical solution temperature (UCST) behavior and allow new features and multipurpose applications.[22,47,56–67] For instance, Perrier and coworkers prepared charged-stabilized core-shell nanoparticles for efficient cell imaging,[22] Huck and coworkers revealed quaternized PDMA grafted on flat surfaces possessed ion-responsive behavior and counterion-dependent wettability,[63,64] Yuan et al. revealed normal and quaternized PDMA grafted graphene oxide had different thermo-dependent behaviors of dispersion and surface wettability due to their LCST or UCST-type thermo-responsiveness,[65] and Ma et al. found mesoporous silica nanoparticles grafted with copolymers with positive charged quaternary amines and polyethylene glycol (PEG) units were liable to exhibit enhanced tumor accumulation and cancer therapy efficacy.[66] At present, most of quaternization reactions are based on macromolecules and small molecules,[68–72] and the examples on quaternization between polymers[73,74] are very limited. Considering the great potential of quaternization to generate complex topological grafts and endow hybrid materials with specific functions via inducing conformational changes, it is urgent to construct solid substrates grafted with novel architectures with quaternization linkages.

Herein we reported efficient synthesis of three types of quaternized polymeric architectures grafted silica via two step reactions (Scheme 1). As a versatile platform for postpolymerization modification, PDMA grafted silica nanoparticles were initially prepared by tandem approach comprising simultaneous alkoxysilane-hydroxyl coupling reaction and RAFT polymerization mediated by a couplable RAFT agent 4-(trimethoxysilyl)benzyl dithiobenzoate (TBDB). On this basis, bromide-functionalized small molecules and polymers were attached onto surface-tethered PDMA backbone to form linear and comblike copolymers grafted silica via "grafting to" method, and tandem quaternization and RAFT process using difunctional 3-bromopropyl 4-benzodithioyl-4-cyanopentanoate (BBCP) were used to generate toothbrushlike copolymers grafted silica. Effects of reaction conditions on grafting density and quaternization efficiency were investigated, and the surface wettability of hybrid films was preliminarily revealed. This study primarily aims at extending the quaternization process to achieve novel ion-bearing macromolecular architectures grafted onto solid substrates, and the resultant silica-polymer hybrids may have a great potential in smart functional materials.

Experimental section

Materials

All monomers were purchased from Sigma-Aldrich, and other chemicals were purchased from Sinopharm Chemical Reagent Co., Ltd. unless other stated. 2-(Dimethylamino)ethyl methacrylate (DMA, 97%) and *tert*-butyl acrylate (*t*BA, 98%) were passed through a basic alumina column to remove the inhibitor, methyl methacrylate (MMA, 99%) and styrene (St, 99%) were distilled from calcium hydride under reduced pressure, and *N*-isopropylacrylamide (NIPAM, 97%) was recrystallized from mixtures of hexane and toluene. Dichloromethane and dioxane were dried and distilled over CaH_2, tetrahydrofuran (THF) and toluene was distilled over sodium and benzophenone, and *N,N*-dimethylformamide (DMF) was dried over $MgSO_4$ and distilled under reduced pressure. 2,2'-Azobis(isobutyronitrile) (AIBN, 99%) was recrystallized twice from ethanol. *N,N*'-Dicyclohexylcarbodiimide (DCC) and 4-dimethylaminopyridine (DMAP) were used as received. Tetraethoxysilane (TEOS, 99%), 3-bromopropanol (97%), 3-bromopropionic acid (98%), benzyl bromide (98%) and 4-(chloromethyl)phenyl trimethoxysilane (90%) were purchased from Alfa Aesar and used as received. 3-Bromopropyl 4-benzodithioyl-4-cyanopentanoate (BBCP)[74] and 4-cyanopentanoic acid dithiobenzoate (4-CPDB)[75] were synthesized and purified according to literature procedures. Bromide-terminated homopolymers PMMA-Br ($M_{n,GPC}$ = 4080, PDI = 1.10), PSt-Br ($M_{n,GPC}$ = 2710, PDI = 1.11), PNIPAM-Br ($M_{n,GPC}$ = 3700, PDI = 1.08) and P*t*BA-Br ($M_{n,GPC}$ = 4180, PDI = 1.12) were prepared by BBCP mediated RAFT polymerization according to previous procedures.[74]

Synthesis of silica nanoparticles

Silica nanoparticles were prepared according to Stöber method.[76,77] A mixture of 282 mL of ethanol and 79.8 mL of water was heated to 45 °C in a water bath pot. After the temperature of the mixture was equilibrated for 30 min, ammonia solution (14.5 mL, 25%) and TEOS (23.2 mL) were added quickly under strong stirring for 5 min. After stirring for 3 h at room temperature, the resulting particles were separated by centrifugation and thoroughly washed to neutral with water using ultrasonication and centrifugation after each step. The particles were dried at 100 °C overnight under ambient air, and 6.22 g of silica nanoparticles were obtained. The average diameter of silica nanoparticles was determined to be about 100 nm by TEM (Fig. 1a), and the BET specific surface area was 36.5 $m^2 g^{-1}$.

Synthesis of 4-(trimethoxysilyl)benzyl dithiobenzoate (TBDB)

To a round flask were added 0.316 g (13.0 mmol) of magnesium rod, 50.0 mL of dry THF and small amount of iodine under nitrogen, and then followed by slow addition of 1.57 g (10.0 mmol) of bromobenzene. The mixture was stirred at 50 °C for 3 h, cooled down, and followed by addition of 1.14 g (15.0 mmol) of dry CS_2. After heating at 45 °C for 10 h, 2.47 g (10.0 mmol) of 4-(chloromethyl)phenyl trimethoxysilane was added to the contents, and the reaction was performed at 45 °C for 20 h. The crude product was cooled and filtered, and concentration of the filtrate afforded 3.60 g (9.88 mmol) of TBDB, which was used as received in this study. ^{1}H NMR ($CDCl_3$): δ 7.98 (d, *J* 7.5, 2H, Ph*H*), 7.61 (d, *J* 7.8, 2H, Ar*H*), 7.52 (t, *J* 6.9, 1H, Ph*H*), 7.41 (t, *J* 8.1, 2H, Ph*H*), 7.37 (d, *J* 7.8, 2H, Ar*H*), 4.60 (s, 2H, CH_2O), 3.62 (s, 9H, CH_3OSi). IR (KBr): 3059, 3019, 2941, 2841, 1654, 1639, 1603, 1445, 1398, 1225, 1191, 1125, 1083, 1045, 879, 812, 761, 726, 687 cm^{-1}.

One-pot synthesis of SiO_2-*g*-PDMA (G1)

To a dried glass tube were added 2.0 g of SiO_2 and 20 mL dioxane, and the mixture was subjected to ultrasonication for 1 h. After that, DMA (31.4 g, 0.20 mol), TBDB (0.73 g, 2.0 mmol), AIBN (68 mg, 0.40 mmol) were added, and dioxane was added to the tube until the total volume was 67 mL. The contents were

This journal is © The Royal Society of Chemistry [year]

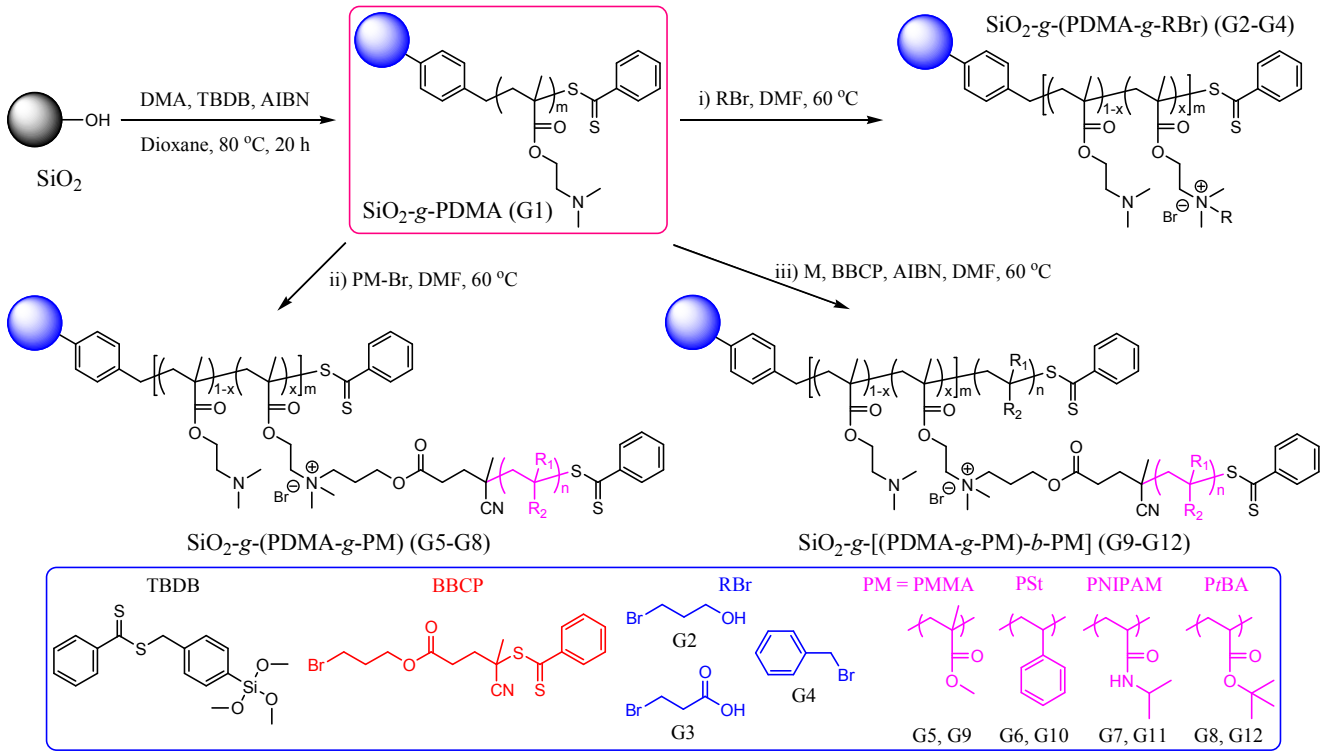

Scheme 1 Synthetic routes to silica nanoparticles grafted with PDMA (SiO_2-*g*-PDMA, G1), quaternized linear copolymers with various functionalities (SiO_2-*g*-(PDMA-*g*-RBr), G2-G4), quaternized comblike copolymers (SiO_2-*g*-(PDMA-*g*-PM), G5-G8) and quaternized toothbrushlike copolymers (SiO_2-*g*-[(PDMA-*g*-PM)-*b*-PM], G9-G12).

degassed with bubbled nitrogen for 30 min, polymerized at 80 °C for 20 h and precipitated into hexane. Monomer conversion was determined to be 97.1% by gravimetry. The reaction mixture was redispersed in 100 mL of THF and subjected to centrifugation. The solution was concentrated and precipitated into hexane to give free polymer. Apparent molecular weight and polydispersity of free PDMA estimated by GPC were $M_{n,GPC}$ = 24400, PDI = 1.75, and ^{1}H NMR analysis ($DP_{PDMA} = I_{2.57}/I_{7.98}$ = 141) gave $M_{n,NMR}$ value of 22500. The crude hybrid sample was thoroughly washed with THF to remove any ungrafted polymer, and 2.3 g of PDMA grafted silica (G1) was collected after centrifugation and vacuum drying. The weight grafting ratio (G_r, defined as weigh ratio of grafted polymer to solid substrate) was calculated as 15.9% by using the equation $G_r = (W_{100,SiO2\text{-}polymer} \times W_{600,SiO2})/(W_{600,SiO2\text{-}polymer} \times W_{100,SiO2}) - 1$, where $W_{100,SiO2\text{-}polymer}$ and $W_{100,SiO2}$ are residual weight of polymer grafted silica and pristine SiO_2 at 100 °C, and $W_{600,SiO2\text{-}polymer}$ and $W_{600,SiO2}$ are residual weight of polymer grafted silica and pristine SiO_2 at 600 °C. Apparent molar grafting ratio ($G_p = G_r/M_n$(g), where M_n(g) was number-average molecular weight of grafted polymer) was estimated to be 7.07 μmol g^{-1}. The G_r and G_p values of other silica-polymer hybrids were calculated by the same equations.

Synthesis of silica nanoparticles grafted with quaternized random copolymers bearing various functionalities (SiO_2-*g*-(PDMA-*g*-RBr), G2-G4)

In this procedure, bromine-containing small molecules were attached onto the side chains of surface-tethered PDMA segments via quaternization. In a typical run (run G2 of Table 1), to a Schlenk tube were added SiO_2-*g*-PDMA (50 mg, 0.044 mmol of DMA unit) and 3-bromopropanol (18 mg, 0.066 mmol) and 2.0 mL DMF under nitrogen, and the contents were heated at 70 °C for 72 h. The reaction mixture was centrifuged and the isolated crude product was subjected to redispersion, centrifugation and thoroughly washed with THF for several times. The hybrid sample was carefully collected and dried under vacuum at 50 °C until constant weight, and 54 mg of silica nanoparticles with 3-bromopropanol modified PDMA grafts (G2) were obtained. The total G_r value of G2 was determined to be 26.6% by TGA analysis, and thus the molar grafting ratio of grafted 3-bromopropanol was deduced to be 770 μmol g^{-1} using the equation $G_{p,A} = (G_r - G_{r,PDMA})/M_{n,A}$ (A = 3-bromopropanol). As 3-bromopropionic acid and benzyl bromide were used for quaternization, quaternized PDMA grafted silica samples G3 and G4 were obtained respectively.

Synthesis of silica nanoparticles grafted with quaternized comblike copolymers (SiO_2-*g*-(PDMA-*g*-PM), G5-G8)

Bromide-terminated polymers synthesized by RAFT polymerization mediated by BBCP were used to graft onto G1 to form the title products. In a typical run (run G5 of Table 1), to a Schlenk tube were added SiO_2-*g*-PDMA (50 mg, 0.044 mmol of DMA unit), PMMA-Br ($M_{n,NMR}$ = 3950, 348 mg, 0.088 mmol) and 2.0 mL of DMF under nitrogen, and the quaternization was performed at 60 °C for 72 h. The reaction mixture was centrifuged, and the isolated crude product was thoroughly washed with toluene and THF. After centrifugation and drying under vacuum, 56 mg of SiO_2-*g*-(PDMA-*g*-PMMA) (G5) was

obtained. The total G_r of G5 was determined to be 34.0% by TGA analysis, and thus the molar grafting ratio of grafted PMMA segments was deduced to be 45.8 μmol g^{-1} using the equation $G_{p,PMMA} = (G_r - G_{r,PDMA})/M_{n,PMMA}$. Other SiO_2-*g*- (PDMA-*g*-PM) samples (PM = PSt (G6), PNIPAM (G7) and P*t*BA (G8)) were prepared according to similar procedures.

Synthesis of silica nanoparticles grafted with quaternized toothbrushlike copolymers (SiO_2-*g*-[(PDMA-*g*-PM)-*b*-PM], G9-G12)

In a typical reaction (run G9 of Table 1), to a Schlenk tube were added SiO_2-*g*-PDMA (50 mg, 0.044 mmol of DMA unit), BBCP (35.2 mg, 0.088 mmol), AIBN (3.0 mg, 0.018 mmol) and MMA (0.66 g, 6.6 mmol), and then DMF was added until the total volume was 3.3 mL. After three freeze-pump-thaw cycles, the tube was subsequently immersed into an oil bath thermostated at 60 °C to conduct graft reaction. The polymerization was performed for 24 h, and the mixture was concentrated and precipitated into cold methanol. Monomer conversion (C%) was determined to be 77% by gravimetry. The mixture of silica-polymer hybrid and free PMMA produced in solution was redispersed in THF. After that, 65 mg of SiO_2-*g*-[(PDMA-*g*-PMMA)-*b*-PMMA] (G9) was recovered by centrifugation and thorough washing using toluene and THF, and free PMMA was isolated by concentration and precipitation into methanol. GPC and ^{1}H NMR analyses of PMMA: $M_{n,GPC}$ = 6170, PDI = 1.11, and $M_{n,NMR}$ = 6400. The total G_r given by TGA analysis was 55.3%, and $G_{p,PMMA}$ by assuming free PMMA and grafted PMMA side chains had same polymerization degree was estimated to be 61.6 μmol g^{-1}. SiO_2-*g*-[(PDMA-*g*-PM)-*b*-PM] samples (PM = PSt (G10), PNIPAM (G11) and P*t*BA (G12)) and other PSt-based hybrids to monitor reaction kinetics during tandem reaction to graft PSt segments were synthesized and purified according to similar procedures.

Hydrolysis of SiO_2-*g*-[(PDMA-*g*-PSt)-*b*-PSt]

To a glass tube were added G10 (50 mg), ethanol (1.0 mL), water (0.2 mL), THF (5 mL) and KOH (100 mg), and then the mixture was refluxed for 40 h. After centrifugation, the solution obtained was concentrated and neutralized with 0.1 M HCl. The crude product was partitioned between water and dichloromethane. After washing with deionized water, the organic layer was collected and precipitated into cold methanol. PSt was isolated and subjected to GPC analysis: $M_{n,GPC}$ = 4040, PDI = 1.10.

Characterization

Apparent molecular weight ($M_{n,GPC}$) and polydispersity (PDI) of PSt, PMMA and P*t*BA were measured on a Waters 150-C gel permeation chromatography (GPC) using three Ultrastyragel columns (pore size 50, 100, and 1000 nm, with molecular weight ranges within 100−600000) with 10 μm bead size at 35 °C. THF was used as an eluent at a flow rate of 1.0 mL min^{-1}, PSt were calibrated with PSt standard samples, and PMMA and P*t*BA were calibrated using PMMA standard samples. $M_{n,GPC}$ and PDI of PDMA and PNIPAM were measured on a Waters 1515 GPC using three MZ-Gel SDplus columns (pore size 10^3, 10^4 and 10^5 Å, with molecular weight ranges within 1000−2000000) with 10 μm bead size at 40 °C. DMF was used as an eluent at a flow rate of 1.0 mL min^{-1}, and the samples were calibrated with PMMA standard samples. ^{1}H NMR spectra (300 MHz) were recorded on a Varian spectrometer at 25 °C using $CDCl_3$ as a solvent. Fourier Transform Infrared (FT-IR) spectra were recorded on a Perkin-Elmer 2000 spectrometer using KBr discs. Specific surface area of silica nanoparticles was determined by the Brunauer–Emmett–Teller (BET) and Non-local Density Functional Theory (NLDFT) methods using N_2 adsorption isotherm measured by a Micrometeritics ASAP 2020 M+C instrument. Dynamic light scattering (DLS) measurements were carried out at 25 °C using Zetasizer Nano-ZS from Malvern Instruments equipped with a 633 nm He–Ne laser using back-scattering detection. The hybid films were prepared by spin-coating method using the solution of silica-polymer hybrids dispersed in THF (c = 1.0 mg mL^{-1}) and a fixed rotation speed of 800 rpm, and static water contact angles (CAs) of pristine and functionalized silicon surfaces were measured on a C201 optical contact angle meter (Solon Information Technology Co., Ltd.) using the sessile drop method. Thermal gravimetric analysis (TGA) was performed using a Perkin-Elmer Pyris 6 TGA instrument with a heating rate of 10 °C min^{-1} under nitrogen. Differential scanning calorimetry (DSC) analysis was performed under a nitrogen atmosphere on Q200 DSC (TA Instruments - Waters LLC) with a heating rate of 10 °C min^{-1}. Transmission electron microscopy (TEM) images were obtained through a Hitachi H-600 electron microscope.

Results and discussion

One-pot synthesis of SiO_2-*g*-PDMA

In traditional graft reaction via "grafting from" approach,[1–6,17–19] hydroxyl-alkoxysilane coupling reaction and postmodification were first used to attach functional initiating sites onto the surface of silica particles, and then followed by polymerization to grow polymeric chains. The stepwise method was efficient to generate silica-polymer hybrids with relatively high grafting density although multistep syntheses were normally necessary. To optimize the synthetic strategy, tandem coupling and RAFT processes were utilized to synthesize silica grafted with PDMA comprising quaternizable tertiary amine functionalities. To this end, silica nanoparticles were prepared according to the Stöber method, and DLS measurement indicated their apparent hydrodynamic diameter (D_h) and particle size distribution (PD) were 128 nm and 0.083 (Fig. S1). TEM image revealed the average diameter of spherical particles was about 100 nm (Fig. 1a). Meanwhile, an alkoxysilane-functionalized RAFT agent 4-(trimethoxysilyl)benzyl dithiobenzoate (TBDB, Fig. S2 and Fig. S3) was synthesized, which acted as both coupling and RAFT agents during the subsequent graft reaction.

To obtain PDMA grafted silica, the graft reaction ($[DMA]_0$:$[TBDB]_0$:$[AIBN]_0$ = 100:1:0.2, $[M]_0$ = 3.0 mol L^{-1}, $m_{Si\text{-}CTA}$:W_{SiO2} = 1.0 mmol g^{-1}) was conducted in dioxane at 80 °C for 20 h. After reaction, free polymer produced in solution was isolated by centrifugation and precipitation, and SiO_2-*g*-PDMA (G1) was recovered by thorough washing, centrifugation and vacuum drying. Apparent molecular weight and polydispersity of free PDMA were estimated to be $M_{n,GPC}$ = 24400 and PDI = 1.75 by GPC analysis (Fig. S4). In ^{1}H NMR spectrum (Fig. S5), characteristic signals were noted at 7.3-8.0 (Ar*H* and Ph*H*), 4.06

This journal is © The Royal Society of Chemistry [year]

Table 1 Results for synthesis of SiO_2-*g*-PDMA (G1), SiO_2-*g*-(PDMA-*g*-A) (G2-G8), and SiO_2-*g*-[(PDMA-*g*-A)-*b*-A] (G9-G12)[a]

run	A	DP_0	$M_{n,GPC}$[b]	PDI[b]	$M_{n,NMR}$[c]	G_r (%)[d]	$G_{p,PDMA}$ (μmol g^{-1})[e]	$G_{p,A}$ (μmol g^{-1})[e]	QE (%)[f]
G1	—	100	24400	1.75	22500	15.9	7.07	0	0
G2	$HOCH_2CH_2CH_2Br$	—	—	—	—	26.6	7.07	770	77.2
G3	$HOOCCH_2CH_2Br$	—	—	—	—	28.0	7.07	791	79.3
G4	$PhCH_2Br$	—	—	—	—	21.7	7.07	339	34.0
G5	PMMA-Br	—	4080	1.10	3950	34.0	7.07	45.8	4.59
G6	PSt-Br	—	2710	1.11	2800	32.6	7.07	58.5	5.98
G7	PNIPAM-Br	—	3700	1.08	3640	37.2	7.07	59.6	5.87
G8	P*t*BA-Br	—	4180	1.12	4020	31.3	7.07	38.3	3.84
G9	PMMA	75	6170	1.11	6400	55.3	7.07	61.6	5.47
G10	PSt	150	3930	1.14	4140	49.2	7.07	80.4	7.36
G11	PNIPAM	75	6670	1.12	6600	52.1	7.07	54.8	4.79
G12	P*t*BA	75	7510	1.14	7100	47.9	7.07	45.1	3.81

[a] Reaction conditions: $[DMA]_0:[TBDB]_0:[AIBN]_0 = 200:1:0.2$, $[M]_0 = 3.0$ mol L^{-1}, $m_{Si\text{-}CTA}:W_{SiO2} = 1.0$ mmol g^{-1}, in dioxane at 80 °C for 20 h (run G1); $[A]_0:[DMA\ unit]_0 = 3$ (runs G2-G4) and 2 (runs G5-G8), $W_{SiO2\text{-}g\text{-}PDMA}:V_{DMF} = 25$ mg mL^{-1}, in DMF at 60 °C for 72 h (runs G2-G8); $[M]_0:[BBCP]_0:[AIBN]_0 = DP_0:1:0.2$, $[BBCP]_0:[DMA\ unit]_0 = 2$, $[M]_0 = 2.0$ mol L^{-1}, in DMF at 60 °C for 24 h (runs G9-G12). [b] Molecular weight and polydispersity estimated by GPC. [c] Molecular weight of free polymer (runs G1 and G9-G12) and PM-Br (runs G5-G8) determined by ^{1}H NMR analysis. [d] Weight grafting ratio determined by TGA. [e] Molar grafting ratio of PDMA ($G_{p,PDMA} = G_{r,PDMA}/M_{n,PDMA}$) and A ($G_{p,A} = (G_r - G_{r,PDMA})/M_{n,A}$) grafted onto silica substrate. [f] Quaternization efficiency (QE = $G_{p,A}/(G_{p,PDMA} \times DP_{PDMA})$ (runs G2-G8) or $(G_{p,A} - G_{p,PDMA})/(G_{p,PDMA} \times DP_{PDMA})$ (runs 9-12)), which was defined as molar ratio of grafted A to total DMA units of SiO_2-*g*-PDMA.

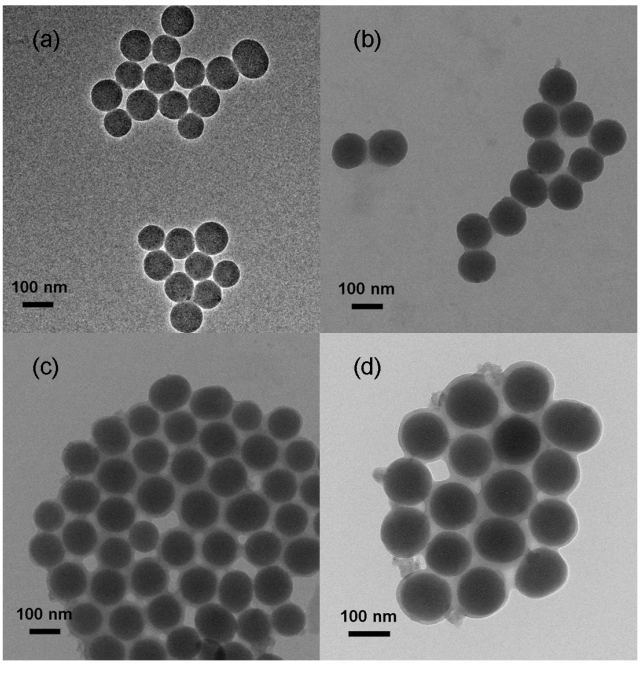

Fig. 1 Typical TEM images of silica nanoparticles (a), SiO_2-*g*-PDMA (G1, b), SiO_2-*g*-(PDMA-*g*-PMMA) (G5, c) and SiO_2-*g*-(PDMA-*g*-PSt) (G6, d). The samples were dispersed in ethanol (a) and THF (b-d) before dropping onto the copper grid coated with carbon.

(CH_2O of PDMA), 3.65 (CH_3OSi), 2.57 (CH_2N of PDMA) and 2.29 ppm ($(CH_3)_2N$ of PDMA). The degree of polymerization ($DP_{PDMA} = I_{2.57}/I_{7.98}$) was calculated as 141, corresponding to $M_{n,NMR}$ value of 22500. From TGA curves of pristine silica and SiO_2-*g*-PDMA (Fig. 2), the weight grafting ratio (G_r) was determined to be 15.9%, and apparent molar grafting ratio ($G_p = G_r/M_n(g)$) was around 7.07 μmol g^{-1} by assuming grafted and free polymers had same molecular weights (Table 1). Considering the BET specific surface area of 36.5 m^2 g^{-1}, the grafting density was deduced to be about 0.117 chain nm^{-2}. The diameter of silica nanoparticles was about 100 nm, and the average size of G1 increased to about 114 nm (Fig. 1b). The surface of G1 was much rougher than pristine silica due to grafting, and careful inspection of TEM image could observe the microdomain originating from grafted PDMA segments. Although the grafting density seemed lower than that obtained by normal "grafting from" approach, it favored the subsequent postpolymerization modification via quaternization due to reduced steric hindrance. Meanwhile, the medium grafting density could be further enhanced as higher ratio of $m_{Si\text{-}CTA}$ to W_{SiO2} was used for the graft reaction. These results confirmed that we could make efficient use of concurrent coupling and RAFT processes to construct PDMA grafted silica.

Synthesis of quaternized linear and comblike copolymers grafted silica via "grafting to" approach

G1 has a large amount of couplable DMA units at the surface of solid substrates, which allows versatile postpolymerization modification in addition to RAFT chain extension

polymerization. In this study, the "grafting to" method is used to attach bromide-functionalized small molecules and polymers onto PDMA backbone to form the target hybrids.

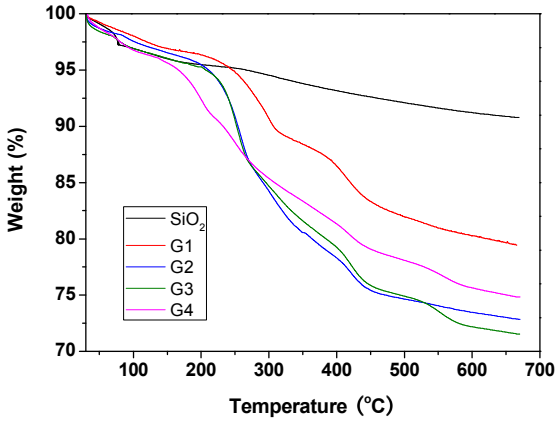

Fig. 2 TGA curves of pristine silica nanoparticles, PDMA grafted silica (G1) and SiO_2-*g*-(PDMA-*g*-RBr) (RBr = 3-bromopropanol (G2), 3-bromopropionic acid (G3) and benzyl bromide (G4).

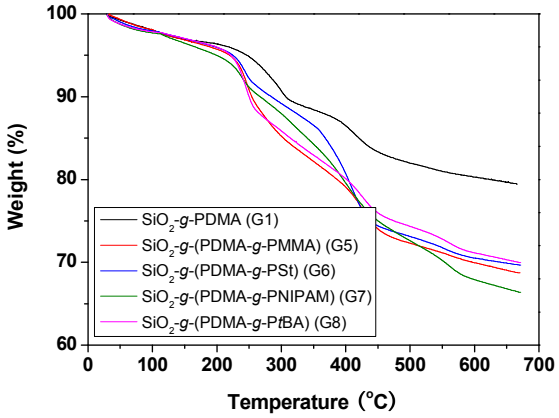

Fig. 3 TGA curves of quaternized comblike copolymers grafted silica (G5-G8) obtained by "grafting to" approach and their precursor G1.

The quaternization process using bromide-containing small molecules (RBr) can introduce various functionalities into surface-tethered PDMA backbone to form silica nanoparticles grafted with quaternized linear random copolymers comprising normal and quaternized DMA units. To this end, 3-bromopropanol, 3-bromopropionic acid and benzyl bromide were chosen as typical agents to react with G1 to introduce reactive or hydrophobic moieties, and SiO_2-*g*-(PDMA-*g*-RBr) samples G2-G4 were obtained. The quaternization reaction ($[RBr]_0$:$[DMA\ unit]_0$ = 3, $W_{SiO2\text{-}g\text{-}PDMA}$:$V_{DMF}$ = 25 mg mL^{-1}) was performed in DMF at 60 °C for 72 h, and the hybrids were isolated by washing and centrifugation. TGA analysis revealed the G_r values were in the range 21.7-28.0% (Fig. 2). Based on the equation $G_{p,RBr} = (G_r - G_{r,PDMA})/M_{n,RBr}$, the molar grafting ratio of bromide agents on silica surface was deduced to be within 339-791 μmol g^{-1}. Therefore, the quaternization efficiency (QE = $G_{p,RBr}/(G_{p,PDMA} \times DP_{PDMA})$ was estimated to be about 34.0-79.3%. The quaternization efficiencies of G2 (RBr = 3-bromopropanol) and G3 (RBr = 3-bromopropionic acid) were similar and higher than that of G4 (RBr = benzyl bromide). Taking account of the microenvironment of heterogeneous reaction and hydrophilic PDMA grafts, this phenomenon could be partly ascribed to enhanced hydrophobicity and steric hindrance of benzyl bromide than other hydrophilic agents. These results indicated most of surface-tethered DMA units could be efficiently quaternized under optimized conditions even if relatively low Br/N feed ratio ($[RBr]_0$:$[DMA]_0$ = 3) was used.

Meanwhile, the quaternization reaction between G1 and bromide-terminated polymers (PM-Br) using a fixed Br/N feed ratio ($[PM\text{-}Br]_0$:$[DMA\ unit]_0$ = 2) was performed in DMF at 60 °C for 72 h, and SiO_2-*g*-(PDMA-*g*-PM) samples (PM = PMMA (G5), PSt (G6), PNIPAM (G7) and P*t*BA (G8)) were obtained. Bromide-terminated homopolymers were prepared by RAFT polymerization of various vinyl monomers mediated by 3-bromopropyl 4-benzodithioyl-4-cyanopentanoate (BBCP), and they had molecular weights ($M_{n,NMR}$) in the range 2800-4020 and polydispersity ranging from 1.08 to 1.12 (Fig. S6). As determined by TGA analysis (Fig. 3), the G_r values of G5-G8 varied from 31.3% to 37.2%, and the G_p values of PM-Br grafted onto silica surface were calculated as 38.3-59.6 μmol g^{-1}. These results revealed that the quaternization efficiency ranged between 3.84% and 5.98%, corresponding to every 17-26 of DMA units grafting with one side chain in the surface-tethered comblike architecture. With increasing weight grafting ratios, the formation of core-shell hybrids could be easily seen from TEM images (c and d of Fig. 1), and the average sizes of comblike copolymers grafted silica increased from 114 nm (G1) to about 125-130 nm (G5 and G6). It should be mentioned that it was quite difficult to form grafted polymer brushes with uniformly distributed side chains. Owing to enhanced steric hindrance, the PM-Br segments may preferentially approach the outlayer DMA units to perform graft reaction, and the grafted side chains on comblike grafts were liable to partly cover the surface of hybrid particles. Consequently, the quaternization process to graft polymeric chains was more difficult to perform than attaching small molecules. Although the "grafting to" method only gave silica-polymer hybrids with loosely grafted comblike copolymers, this approach allowed facile synthesis of the target hybrids with variable chemical and weight compositions and tunable chain length of pendent chains.

The above-mentioned results indicated that bromide-functionalized small molecules and polymers could be successfully grafted onto surface-tethered PDMA backbone to form ion-bearing linear and comblike copolymers grafted silica, and the quaternization efficiency could be potentially adjusted by changing reaction conditions.

Synthesis of quaternized toothbrushlike copolymers grafted silica via tandem quaternization and RAFT process

One-pot method comprising concurrent coupling reaction and controlled radical polymerization has been proven efficient to generate well-defined polymers grafted solid substrates such as silica particles and graphene oxide.[16,30–32] Our previous studies revealed quaternization reaction and RAFT polymerization could

This journal is © The Royal Society of Chemistry [year]

be simultaneously conducted to construct complex macromolecular architectures such as miktoarm star and toothbrushlike copolymers.[72–74] Herein tandem quaternization and RAFT process were used to generate toothbrushlike copolymers grafted silica, in which the side chains were formed during concurrent coupling and polymerization based on BBCP, and the handle comprising linear chains was generated by chain extension polymerization mediated by the terminal dithiobenzoate moieties of PDMA grafts. The tandem approach comprising both "grafting to" and "grafting from" processes. The former was used to attach BBCP or BBCP-based RAFT-generated polymers onto side chains of surface-tethered DMA units, and the latter was applied to grow side chains grafted onto PDMA backbone and linear block to form toothbrushlike copolymers.

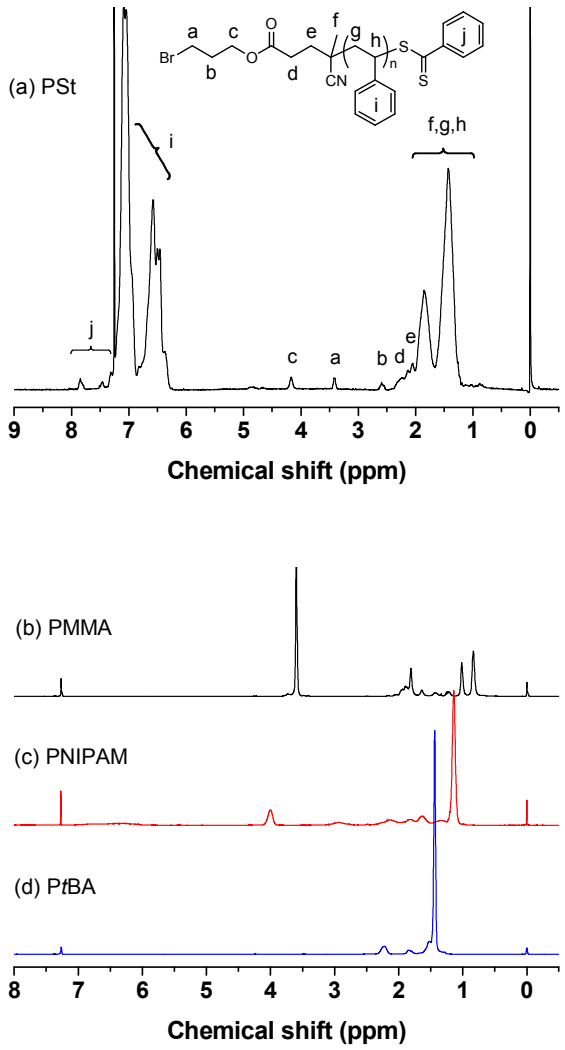

Fig. 4 ^{1}H NMR spectra of free PM samples produced in solution during tandem graft reaction.

During SI-RAFT, free chain transfer agents are usually utilized to improve the controllability on molecular weight and polydispersity of surface-grafted polymeric chains. Herein bromide-functionalized chain transfer agent BBCP acted as both couplable and sacrificial RAFT agent. The former could be grafted onto surface-tethered PDMA backbone via quaternization and grow side chains via RAFT mechanism, and the latter could afford efficient control over chain length and molecular weight distribution of RAFT generated pendent chains and linear handle. With a fixed Br/N ratio ($[BBCP]_0$:$[DMA\ unit]_0$ = 2), the graft reaction of various vinyl monomers was conducted in DMF at 60 °C for 24 h. Free polymers produced in solution were isolated by centrifugation, concentration and precipitation into methanol (for PMMA and PSt), diethyl ether (for PNIPAM) and water/methanol mixture (1:1, v/v, for P*t*BA), and silica nanoparticles grafted with toothbrushlike copolymers SiO_2-*g*-[(PDMA-*g*-PM)-*b*-PM] (PM = PMMA (G9), PSt (G10), PNIPAM (G11) and P*t*BA (G12)) were recovered by centrifugation and thorough washing with toluene and THF.

In ^{1}H NMR spectra of free polymers (Fig. 4), the signals of characteristic protons in polymer segments appeared at 3.60 (CH_3O of PMMA), 6.2-7.2 (Ph*H* of PSt), 4.01 (C*H* of PNIPAM), 2.23 (C*H* of P*t*BA) and 1.44 ppm (CH_3 of P*t*BA), and typical signals originating from chain ends were noted at 7.3-8.0 (Ph*H* of terminal PhC(=S)S), 4.24 (terminal CH_2O) and 3.47 ppm (terminal CH_2Br). On this basis, number-average molecular weights determined by ^{1}H NMR ($M_{n,NMR}$) were obtained by comparing integrated signal areas of protons in polymer chain and end group. GPC analysis revealed various bromide-terminated homopolymers had molecular weight ($M_{n,GPC}$) within the range 3930-7510, and their polydispersity indices were relatively low (PDI = 1.11-1.14, Fig. 5). By assuming that all the RAFT agents had quantitatively participated in RAFT process to generate polymer segments and free and grafted PM segments had same chain length, theoretical molecular weights ($M_{n,th}$) of free polymers were calculated as 6180 (PMMA, 77% conversion), 3990 (PSt, 23% conversion), 6330 (PNIPAM, 70% conversion) and 7020 (P*t*BA, 68% conversion). The $M_{n,th}$ and $M_{n,NMR}$ values were roughly similar ($M_{n,th}/M_{n,NMR}$ = 0.96-0.98), which revealed that most of BBCP had participated in RAFT process during graft reaction no matter it was grafted onto the PDMA backbone or present in solution.

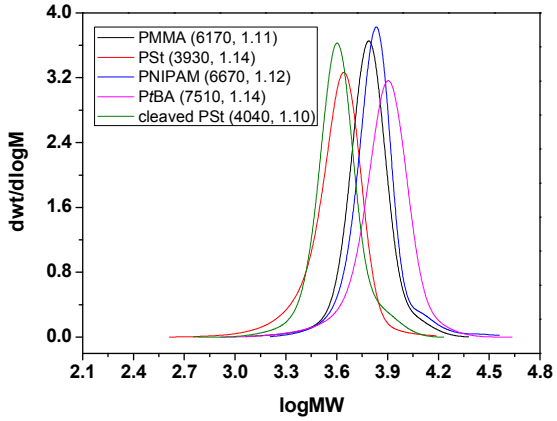

Fig. 5 GPC traces of free polymers produced in solution during tandem graft reaction and cleaved PSt isolated from hydrolysis of SiO_2-*g*-[(PDMA-*g*-PSt)-*b*-PSt] (G10).

As well documented, free and grafted polymers usually possessed similar molecular weights as surface-supported RAFT polymerization was conducted in the presence of suitable amount of sacrificial RAFT agent via "grafting from" approach.[16–19,32] In this study, the reaction system was more complex than normal SI-RAFT process since two types of reactive sites comprising side chains and chain end of PDMA backbone were involved, and the reactive sites in pendent chains of PDMA backbone could be formed via two kinds of quaternization reactions between PDMA backbone and bromide-functionalized RAFT agent (either BBCP or BBCP-based macro CTA). In the first mode, BBCP was initially tethered to PDMA backbone via quaternization, and then followed by surface-supported RAFT process to grow side chains. In the second mode, BBCP mediated RAFT polymerization was performed in solution and afforded bromide-bearing macro RAFT agent (free polymer), and then quaternization and RAFT processes were performed simultaneously. In theory, two modes are concurrent at the early stage of polymerization, the second mode plays a critical role once all the dithiobenzoate moieties have participated in the RAFT process, and the quaternization between DMA units and free polymers will be continuously conducted until either all the DMA units are fully covered by grafted chains or free polymers formed in solution are too bulky to approach DMA units to be quaternized. Owing to the complex reaction processes, it is necessary to understand the uniformity of chain length of grafted side chains and the relationship between polymerization degrees of free and grafted polymeric chains. In addition, it is also important to reveal the evolution of grafting density of surface-tethered toothbrushlike copolymers with reaction time. Profound understanding of these issues is helpful to optimize tandem approach to generate well-defined toothbrushlike copolymers grafted silica.

To reveal if free and grafted chains had similar chain length, G10 (PM = PSt) was subjected to hydrolysis, and the cleaved PSt was isolated. GPC analysis revealed the $M_{n,GPC}$ and PDI values of cleaved PSt were 4040 and 1.10, and the corresponding values of free PSt were 3930 and 1.14 (Fig. 5). The M_n values of free and grafted PSt chains were similar and close to the theoretical value ($M_{n,th}$ = 3990), and their polydispersity indices were around 1.1, as expected from a controlled radical polymerization system. Careful inspection of GPC traces revealed free polymer was liable to exhibit more pronounced tailing than cleaved PSt in GPC trace, whilst the cleaved sample showed a notable shoulder (about 5% signal area) corresponding to radical coupling product. These results indicated that the radical disproportionation termination on the surface of solid substrates was negligible during surface-initiated graft reaction, whilst the radical coupling termination was unavoidable due to relatively high chain radical concentration around PDMA backbone and surface confined microenvironment to generate chain propagation. Although the peak molecular weight of cleaved PSt (M_p = 4000) was slightly lower than that of free PSt (M_p = 4380), the chain lengths of free and grafted PSt segments were roughly comparable since cleaved PSt lacked the end groups originating from BBCP. Therefore, free polymers and grafted pendent chains had similar degree of polymerization although they were prepared by either homogeneous or heterogeneous RAFT polymerization.

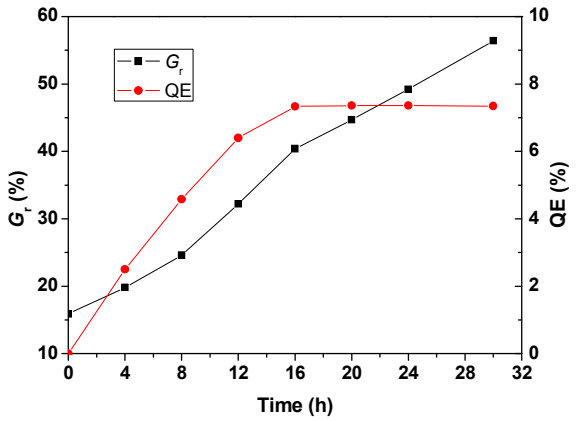

Fig. 6 Influence of reaction time on weight grafting ratio (G_r) and quaternization efficiency (QE) during tandem method to synthesize SiO_2-*g*-[(PDMA-*g*-PSt)-*b*-PSt].

To further understand the evolution of detailed graft process with time, tandem graft reactions to introduce PSt chains were conducted in DMF at 60 °C for different times, and the reaction kinetics was monitored. The G_r values of hybrid samples were determined by TGA analysis, and molecular weights of free PSt were estimated by GPC measurement. As monomer conversion increased from 2.8% (t = 4 h) to 28.3% (t = 30 h), $M_{n,GPC}$ increased from 1180 to 4980, and the polydispersity was gradually decreased from 1.43 to 1.13. As expected, the $M_{n,NMR}$ values of free polymers were usually close to the theoretical values (Table S1). By assuming that free and grafted PSt chains had same molecular weights, the quaternization efficiency was calculated using the equation $QE = (G_{p,PSt} - G_{p,PDMA})/(G_{p,PDMA} \times DP_{PDMA})$, where $G_{p,PSt}$ was apparent molar grafting ratio of grafted PSt estimated by the equation $G_{p,PSt} = (G_r - G_{r,PDMA})/M_{n,PSt}$. Dependence of the total weight grafting ratio and QE on time is plotted in Fig. 6. As the graft reaction was performed for 30 h, G_r was liable to increase from 15.9% (t = 0) to 56.4% (t = 30 h), and QE was gradually enhanced to about 7.4% in 16 h and tended to be constant with prolonging time, revealing that the quaternization process almost reached to a maximum as $M_{n,NMR}$ of PSt was about 3060. Two factors could account for this phenomenon. On one hand, the enhanced chain length of macro RAFT agent (free polymer) obtained with extended time was liable to prevent the bromide functionality from approaching DMA units to perform quaternization, and this tendency became more pronounced as polymeric chains were long enough. On the other hand, the surface graft reaction was conducted in a confined microenvironment, and the presence of grafted PSt chains on side chains and linear block of toothbrush copolymers could significantly shield the remaining DMA units from quaternization. Therefore, the quaternization process could not conduct any more as the chain length of free polymers reached to a critical value resulting in significant shielding effect. On the contrary, the graft reaction could smoothly perform until relatively high monomer conversion was reached since monomers were liable to diffuse freely to approach chain radicals at silica surface to activate RAFT process.

This journal is © The Royal Society of Chemistry [year]

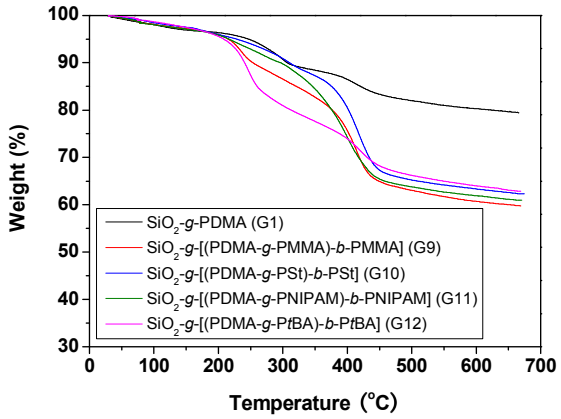

Fig. 7 TGA curves of quaternized toothbrushlike copolymers grafted silica (G9-G12) obtained by tandem quaternization and RAFT process and their precursor G1.

As compared with comblike copolymers grafted silica obtained by "grafting to" approach, no remarkable enhancement in quaternization efficiency was noted in G9-G12 prepared via tandem method (Table 1). Based on TGA analysis (Fig. 7), the G_r values were determined to be 47.9-55.3%, and the QE was estimated within the range 3.81-7.36% by assuming free polymers, grafted side chains and linear block generated by graft reaction had same chain length. These results indicated the grafting density of comblike block was about 14-26 DMA units per grafted chain, which belonged to loosely grafted system. G10 with PSt grafted chains had higher QE than other hybrids containing PMMA, PNIPAM and P*t*BA segments, which could be mainly ascribed to the lowered polymerization kinetics in addition to other factors such as different molecular weight and chain rigidity. In one-pot method to prepare the hybrids, slower RAFT process was liable to generate shorter chain length of free polymer in a fixed time period. Consequently, the probability for continuous quaternization was enhanced, and the efficient time for quaternization was also extended, resulting in relatively high QE during tandem graft reaction.

The afore-mentioned results indicated the quaternization and RAFT processes could be tandem conducted to afford the target toothbrushlike copolymers grafted silica. The grafted chains usually had controlled molecular weight and relatively low polydispersity, and the quaternization efficiency could be roughly adjusted by control over reaction conditions and choosing different types of monomers.

Surface wettability of hybrid films

Besides surface roughness, the surface wettability of hybrid films may be affected by other factors such as macromolecular architecture, grafting density, chemical composition, phase transition, and degree of quaternization. PDMA (normal and quaternized) and PNIPAM polymer segments usually exhibit a temperature-dependent solubility, and thus silica nanoparticles grafted with quaternized polymers potentially possess thermo-responsive surface wettability.

For SiO_2-*g*-PDMA, the glass transition temperature (T_g) was determined by DSC, and LCST was measured by DLS analysis. DSC results revealed the T_g values were about 23.5 °C (free PDMA) and 26.0 °C (G1), and thus surface-tethered PDMA chains were "frozen" at low temperature (T < 20 °C), partly relaxed at 25 °C, and completely relaxed at a temperature beyond 32 °C (Fig. S9). The glass transition of polymer grafted solid substrate was very complex. The covalent bonds bridged solid substrate and surface-tethered polymeric chains usually led to increasingly confined chain movement, resulting in enhanced T_g. On the other hand, the number of end groups in silica-polymer hybrids was much higher than free polymer, which was liable to reduce T_g. In this study, T_g(G1) was slightly higher than T_g(PDMA), revealing the former played more important role in affecting the glass transition. DLS measurement indicated the apparent hydrodynamic diameter (D_h) of G1 was liable to increase at about 44 °C due to the hydrophilic to hydrophobic phase transition of PDMA segments (Fig. 8). With increasing temperature, the pH value of G1 aqueous solution was only slightly decreased from 7.85 (25 °C) to 7.72 (40 °C) and 7.45 (50 and 60 °C), and thus the enhanced size of G1 dispersed in aqueous solution was primarily attributed to the phase transition.

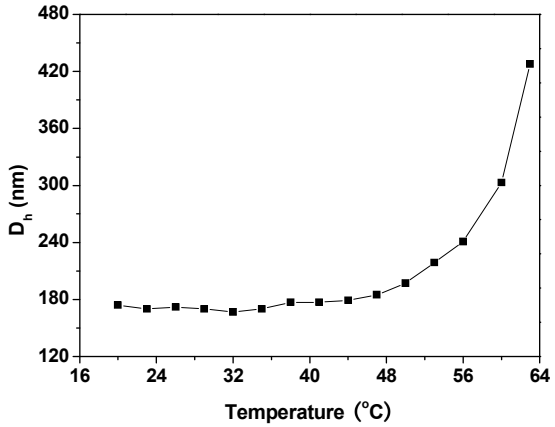

Fig. 8 Influence of temperature on apparent hydrodynamic diameter (D_h) of SiO_2-*g*-PDMA dispersed in aqueous solution (*c* = 0.50 mg mL^{-1}).

On this basis, water contact angles (CAs) of hybrid films at 25 and 50 °C were measured (Table 2), and PM-Br films were also subjected to CA measurement to reveal the influence of grafted PM segments on surface property of hybrid films comprising comblike architecture. The CA values of G1 film were about 56.7° (25 °C) and 71.6° (50 °C), and the CA difference (ΔCA = CA(50 °C) – CA(25 °C)) could reach up to 14.9° due to the increased hydrophobicity of PDMA grafts at a temperature higher than LCST (about 44 °C). This phenomenon could be primarily attributed to the change in temperature-induced chain conformations, in which surface-tethered PDMA chains were liable to adopt random coil conformation at room temperature because of hydrogen bonding interactions, and they were converted into collapsed conformation at high temperature (T > LCST) due to weakened interactions. G2-G4 films grafted with quaternized linear copolymers had CA values within the range

Table 2 Influence of temperature on the water contact angles (CAs) of various composite or polymer films

sample	Type	A	CA (^{o}, 25 ^{o}C)	CA (^{o}, 50 ^{o}C)	ΔCA (^{o})
G1	SiO_2-*g*-PDMA	—	56.7 ± 2.0	71.6 ± 1.7	14.9
G2	SiO_2-*g*-(PDMA-*g*-A)	$HOCH_2CH_2CH_2Br$	55.7 ± 2.4	39.0 ± 1.0	-16.7
G3	SiO_2-*g*-(PDMA-*g*-A)	$HOOCCH_2CH_2Br$	41.5 ± 2.5	30.2 ± 1.4	-11.3
G4	SiO_2-*g*-(PDMA-*g*-A)	$PhCH_2Br$	70.2 ± 1.8	54.7 ± 2.4	-15.5
G5	SiO_2-*g*-(PDMA-*g*-A)	PMMA-Br	50.2 ± 2.5	44.6 ± 2.2	-5.6
G6	SiO_2-*g*-(PDMA-*g*-A)	PSt-Br	67.3 ± 2.1	59.8 ± 2.7	-7.5
G7	SiO_2-*g*-(PDMA-*g*-A)	PNIPAM-Br	21.3 ± 1.9	35.2 ± 2.2	13.9
G8	SiO_2-*g*-(PDMA-*g*-A)	P*t*BA-Br	65.8 ± 2.6	56.6 ± 1.8	-9.2
G9	SiO_2-*g*-[(PDMA-*g*-A)-*b*-A)]	PMMA	64.0 ± 2.8	58.1 ± 1.5	-5.9
G10	SiO_2-*g*-[(PDMA-*g*-A)-*b*-A)]	PSt	89.1 ± 3.3	85.4 ± 2.4	-3.7
G11	SiO_2-*g*-[(PDMA-*g*-A)-*b*-A)]	PNIPAM	30.7 ± 2.4	48.2 ± 1.8	17.5
G12	SiO_2-*g*-[(PDMA-*g*-A)-*b*-A)]	P*t*BA	73.6 ± 3.5	70.3 ± 2.3	-3.3
PMMA-Br	Homopolymer	—	75.8 ± 1.5	74.2 ± 2.6	-1.6
PSt-Br	Homopolymer	—	90.9 ± 2.2	91.8 ± 2.7	0.9
PNIPAM-Br	Homopolymer	—	32.6 ± 1.3	57.1 ± 2.5	24.5
P*t*BA-Br	Homopolymer	—	86.7 ± 1.6	80.5 ± 2.1	-6.2

41.5-70.2^o at 25 ^{o}C and 30.2-54.7^o at 50 ^{o}C, and ΔCA ranged between -11.3^o and -16.7^o. The surface of G2-G4 films at 50 ^{o}C was more hydrophilic, which could be possibly ascribed to the more stretching conformation. The quaternized DMA units could interact with each other via ionic interactions to form compact conformation at low temperature, and they tended to adopt more expanding conformation at higher temperature.[63–65] Consequently, the probability for hydrophilic quaternized moieties to contact water droplets at 50 ^{o}C was significantly increased due to accelerated chain movement and stretching conformation, resulting in increasingly hydrophilic surface property. For SiO_2-*g*-(PDMA-*g*-PM) (G5-G8) hybrid films with quaternized comblike grafts, the CA values at 25 ^{o}C varied from 21.3^o to 67.3^o, which were lower than those of homopolymer (CA = 75.8^o (PMMA-Br), 90.9^o (PSt-Br), 32.6^o (PNIPAM-Br), and 86.7^o (P*t*BA-Br)) films, revealing both quaternized groups and grafted chains could affect the surface wettability. When the temperature was increased to 50 ^{o}C, the surface of G5, G6 and G8 films became more or less hydrophilic (ΔCA = -5.6^o ~ -9.2^o) possibly originating from hydrophobic to hydrophilic transition of quaternized groups, whilst PNIPAM-bearing hybrid film was increasingly hydrophobic (ΔCA = 13.9^o) due to the hydrophilic to hydrophobic phase transition of PNIPAM segments (T > LCST). For SiO_2-*g*-[(PDMA-*g*-PM)-*b*-PM] (G9-G12) films with toothbrushlike copolymers, their CA values ranged between 30.7^o -89.1^o at ambient temperature, which were close to those of their corresponding PM homopolymer films since the inner PDMA backbone was surrounded by grafted PM chains. At a higher temperature (T = 50 ^{o}C), the CA values of G9, G10 and G12 films were slightly decreased (ΔCA = -3.3^o ~ -5.9^o), whilst PNIPAM-based G11 film became more hydrophobic (ΔCA = 17.5^o).

These preliminary results revealed the surface wettability of quaternized hybrid films could be tuned in a wide range (CA(25 ^{o}C) = 21.3^o ~ 89.1^o, CA(50 ^{o}C) = 30.2^o ~ 85.4^o), and all the hybrid films exhibited more or less thermo-dependent surface wettability. As temperature increased from 25 to 50 ^{o}C, PNIPAM-bearing hybrid films were more hydrophobic due to hydrophilic to hydrophobic transition of PNIPAM segments, and other quaternized hybrid films modified with small molecules and polymer chains became more or less hydrophilic due to the hydrophobic to hydrophilic transition of quaternized moieties. The latter can be affected by some factors such as quaternization degree, topology and chain rigidity due to their influence on macromolecular conformation.

Conclusions

We have demonstrated that the combination of alkoxysilane-hydroxyl coupling reaction, quaternization process and RAFT polymerization could efficiently afford three types of topological copolymers grafted silica. Simultaneous coupling and RAFT processes were used to generate PDMA grafted silica with a grafting density of 0.117 chain nm^{-2}. On this basis, the quaternization reaction between G1 and bromide-functionalized small molecules / polymers gave silica nanoparticles grafted with quaternized linear and comblike copolymers, and tandem approach using BBCP afforded quaternized toothbrushlike copolymers grafted silica. Free polymers and grafted side chains produced during tandem reactions had comparable molecular weight and relatively low polydispersity, evident from selective hydrolysis, GPC and ^{1}H NMR analyses. Owing to enhanced steric hindrance, the quaternization efficiency to attach small molecules (QE = 34-79%) was much higher than that to graft

This journal is © The Royal Society of Chemistry [year]

polymeric chains (QE = 3.8-7.4%). Our preliminary results revealed the surface wettability of hybrid films was dependent on some factors such as macromolecular architecture, quaternization degree, chemical composition and temperature. As temperature increased from 25 to 50 ^{o}C, G1, G7 and G11 films with thermo-sensitive PDMA and PNIPAM segments exhibited enhanced water contact angles (ΔCA = 13.9^{o} ~ 17.5^{o}), whilst other hybrid films were more hydrophilic (ΔCA = -3.3^{o} ~ -16.7^{o}), revealing the thermo-dependent surface wettability of hybrid materials. Our study affords a versatile method comprising two step reactions to construct quaternized linear, comblike and toothbrushlike copolymers grafted solid substrates, which is of some advantages such as straightforward synthesis, minimal reaction steps, and mild conditions. Owing to remarkable thermo-responsive surface wettability, the quaternized hybrids may have a great potential as smart surface and interface materials in addition to antibacterial materials.

Acknowledgements

This work was financially supported by the National Natural Science Foundation of China (Grants 21274096 and 21474070), and the Project Funded by the Priority Academic Program Development of Jiangsu Higher Education Institutions.

Notes and references

Suzhou Key Laboratory of Macromolecular Design and Precision Synthesis, Jiangsu Key Laboratory of Advanced Functional Polymer Design and Application, College of Chemistry, Chemical Engineering and Materials Science, Soochow University, Suzhou 215123, China. Tel: +86-512-65882045; Fax: +86-512-65882045; E-mail: *ylzhao@suda.edu.cn*

† Electronic Supplementary Information (ESI) available: [^{1}H NMR and IR spectra, GPC traces, DLS plots, and DSC curves]. See DOI: 10.1039/b000000x/

1 G. J. de A. A. Soler-Illia, C. Sanchez, B. Lebeau and J. Patarin, *Chem. Rev.*, 2002, **102**, 4093–4138.
2 G. Kickelbick, *Prog. Polym. Sci.*, 2003, **28**, 83–114.
3 B. Radhakrishnan, R. Ranjan and W. J. Brittain, *Soft Matter,* 2006, **2**, 386–396.
4 Y. Tsujii, K. Ohno, S. Yamamoto, A. Goto and T. Fukuda, *Adv. Polym. Sci.* 2006, **197**, 1–45.
5 J. Moraes, K. Ohno, T. Maschmeyer and S. Perrier, *Chem. Commun.*, 2013, **49**, 9077–9088.
6 B. Zhao and L. Zhu, *Macromolecules*, 2009, **42**, 9369–9383.
7 A. Olivier, F. Meyer, J. M. Raquez, P. Damman and P. Dubois, *Prog. Polym. Sci.*, 2012, **37**, 157–181.
8 J. P. Deng, L. F. Wang, L. Y. Liu and W. T. Yang, *Prog. Polym. Sci.*, 2009, **34**, 156–193.
9 R. Barbey, L. Lavanant, D. Paripovic, N. Schuwer, C. Sugnaux, S. Tugulu and H. A. Klok, *Chem. Rev.*, 2009, **109**, 5437–5527.
10 T. Chen, I. Amin and R. Jordan, *Chem. Soc. Rev.*, 2012, **41**, 3280–3296.
11 N. Zydziak, B. Yameen and C. Barner-Kowollik, *Polym. Chem.*, 2013, **4**, 4072–4086.
12 H. Jiang and F. J. Xu, *Chem. Soc. Rev.*, 2013, **42**, 3394–3426.
13 R. Francis, N. Joy, E. P. Aparna and R. Vijayan, *Polym. Rev.*, 2014, **54**, 268–347.
14 C. M. Hui, J. Pietrasik, M. Schmitt, C. Mahoney, J. Choi, M. R. Bockstaller and K. Matyjaszewski, *Chem. Mater.*, 2014, **26**, 745–762.
15 Y. Li, T. M. Krentz, L. Wang, B. C. Benicewicz and L. S. Schadler, *ACS Appl. Mater. Interfaces*, 2014, **6**, 6005–6021.
16 R. Ranjan and W. J. Brittain, *Macromol. Rapid Commun.*, 2007, **28**, 2084–2089.
17 R. Ranjan and W. J. Brittain, *Macromol. Rapid Commun.*, 2008, **29**, 1104–1110.
18 C. Z. Li and B. C. Benicewicz, *Macromolecules,* 2005, **38**, 5929–5936.
19 C. Z. Li, J. Han, C. Y. Ryu and B. C. Benicewicz, *Macromolecules*, 2006, **39**, 3175−3183.
20 Y. L. Zhao and S. Perrier, *Macromolecules*, 2006, **39**, 8603–8608.
21 K. Ohno, Y. Ma, Y. Huang, C. Mori, Y. Yahata, Y. Tsujii, T. Maschmeyer, J. Moraes and S. Perrier, *Macromolecules*, 2011, **44**, 8944–8953.
22 J. Moraes, K. Ohno, T. Maschmeyer and S. Perrier, *Chem. Mater.*, 2013, **25**, 3522–3527.
23 M. H. Stenzel, L. Zhang and W. T. S. Huck, *Macromol. Rapid Commun.,* 2006, **27**, 1121–1126.
24 R. Rotzoll and P. Vana, *J. Polym. Sci. Part A: Polym. Chem.,* 2008, **46**, 7656–7666.
25 X. Huang, D. Appelhans, P. Formanek, F. Simon and B. Voit, *Macromolecules,* 2011, **44**, 8351–8360.
26 J. T. Sun, J. G. Piao, L. H. Wang, M. Javed, C. Y. Hong and C. Y. Pan, *Macromol. Rapid Commun.*, 2013, **34**, 1387–1394.
27 Y. K. Huang, Q. Liu, X. D. Zhou, S. Perrier and Y. L. Zhao, *Macromolecules,* 2009, **42**, 5509–5517.
28 Y. K. Huang, T. T. Hou, X. Q. Cao, S. Perrier and Y. L. Zhao, *Polym. Chem.*, 2010, **1**, 1615–1623.
29 T. T. Hou, P. P. Zhang, X. D. Zhou, X. Q. Cao and Y. L. Zhao, *Chem. Commun.*, 2010, **46**, 7397–7399.
30 G. D. Zhao, P. P. Zhang, C. B. Zhang and Y. L. Zhao, *Polym. Chem.*, 2012, **3**, 1803–1812.
31 C. N. Ye, W. N. Qi, X. H. Yu, P. P. Zhang, T. T. Hou and Y. L. Zhao, *Front. Chem. China*, 2011, **6**, 213–220.
32 K. Jiang, C. N. Ye, P. P. Zhang, X. S. Wang and Y. L. Zhao, *Macromolecules*, 2012, **45**, 1346–1455.
33 S. Mahouche, N. Mekni, L. Abbassi, P. Lang, C. Perruchot, M. Jouini, F. Mammeri, M. Turmine, H. Ben Romdhane and M. M. Chehimi, *Surf. Sci.*, 2009, **603**, 3205–3211.
34 S. Gam-Derouich, B. Carbonnier, M. Turmine, P. Lang, M. Jouini, D. Ben Hassen-Chehimi and M. M. Chehimi, *Langmuir*, 2010, **26**, 11830–11840.
35 Z. Zhang, M. L. Chen, X. D. Cheng, Z. G. Shi, B. F. Yuan and Y. Q. Feng, *J. Chromatogr. A*, 2014, **1351**, 96–102.
36 M. Vamvakaki, N. C. Billingham and S. P. Armes, *Macromolecules*, 1999, **32**, 2088–2090.
37 S. B. Lee, A. J. Russell and K. Matyjaszewski, *Biomacromolecules*, 2003, **4**, 1386–1393.
38 X. Liu, P. H. Ni, J. L. He and M. Z. Zhang, *Macromolecules*, 2010, **43**, 4771–4781.
39 W. Agut, A. Brûlet, C. Schatz, D. Taton and S. Lecommandoux, *Langmuir*, 2010, **26**, 10546–10554.
40 Q. J. Chen, X. T. Cao, H. Liu, W. Zhou, L. J. Qin and Z. S. An. *Polym. Chem*., 2013, **4**, 4092–4102.
41 Q. L. Li, C. Q. Gao, S. T. Li, F. Huo and W. Q. Zhang, *Polym. Chem.*, 2014, **5**, 2961–2972.
42 B. J. Gao, Y. X. Chen and Z. G. Zhang, *Appl. Surf. Sci.*, 2010, **257**, 254–260.
43 L. L. Zhou, W. Z. Yuan, J. Y. Yuan and X. Y. Hong, *Mater. Lett.*, 2008, **62**, 1372–1375.
44 H. X. Cheng, S. A. Xie, Y. F. Zhou, W. Huang, D. Y. Yan, J. T. Yang and B. Ji, *J. Phys. Chem. B*, 2010, **114**, 6291–6299.
45 T. Saigal, H. C. Dong, K. Matyjaszewski and R. D. Tilton, *Langmuir*, 2010, **26**, 15200–15209.
46 Z. X. Dong, H. Wei, J. Mao, D. P. Wang, M. Q. Yang, S. Q. Bo and X. L. Ji, *Polymer*, 2012, **53**, 2074–2084.
47 Z. X. Dong, J. Mao, D. P. Wang, M. Q. Yang, W. C. Wang, S. Q. Bo and X. L. Ji, *Macromol. Chem. Phys.*, 2014, **215**, 111–120.
48 J. Y. Yuan, F. Schacher, M. Drechsler, A. Hanisch, Y. Lu, M. Ballauff and A. H. E. Müller, *Chem. Mater.*, 2010, **22**, 2626–2634.
49 W. J. Zhang, C. Y. Hong and C. Y. Pan, *J. Mater. Chem. A*, 2014, **2**, 7819–7828.
50 A. P. Majewski, U. Stahlschmidt, V. Jérôme, R. Freitag, A. H. E. Müller and H. Schmalz, *Biomacromolecules*, 2013, **14**, 3081–3090.

51 H. C. Lee, H. Y. Hsueh, U. S. Jeng and R. M. Ho, *Macromolecules*, 2014, **47**, 3041–3051.
52 T. Sun, Y. F. Zhang, C. L. Chen, X. Z. Gong and J. Q. Meng, *Chinese J. Polym. Sci.*, 2014, **32**, 880–891.
53 F. Schacher, M. Ulbricht and A. H. E. Müller, *Adv. Funct. Mater.*, 2009, **19**, 1040–1045.
54 Y. F. Yang, L. S. Wan and Z. K. Xu, *J. Membr. Sci.*, 2009, **326**, 372–381.
55 R. H. Du, X. S. Feng and A. Chakma, *J. Membr. Sci.*, 2006, **279**, 76–85.
56 F. A. Plamper, A. Schmalz, M. Ballauff and A. H. E. Müller, *J. Am. Chem. Soc.*, 2007, **129**, 14538–14539.
57 E. Karjalainen, V. Aseyev and H. Tenhu, *Macromolecules*, 2014, **47**, 7581–7587.
58 A. Housni and Y. Zhao, *Langmuir*, 2010, **26**, 12933–12939.
59 W. Z. Yuan, H. Zou, W. Guo, A. Wang and J. Ren, *J. Mater. Chem.*, 2012, **22**, 24783–24791.
60 E. Karjalainen, V. Aseyev and H. Tenhu, *Macromolecules*, 2014, **47**, 2103–2111.
61 S. H. Jung and H. I. Lee, *Bull. Korean Chem. Soc.*, 2014, **35**, 501–504.
62 S. Sanjuan, P. Perrin, N. Pantoustier and Y. Tran, *Langmuir*, 2007, **23**, 5769–5778.
63 S. Moya, O. Azzaroni, T. Farhan, V. L. Osborne and W. T. S. Huck, *Angew. Chem., Int. Ed.*, 2005, **44**, 4578–4581.
64 O. Azzaroni, A. A. Brown and W. T. S. Huck, *Adv. Mater.*, 2007, **19**, 151–154.
65 W. Z. Yuan, J. J. Wang, T. X. Shen and J. Ren, *Mater. Lett.*, 2013, **107**, 243–246.
66 M. Ma, S. G. Zheng, H. R. Chen, M. H. Yao, K. Zhang, X. Q. Jia, J. Mou, H. X. Xu, R. Wu and J. L. Shi, *J. Mater. Chem. B*, 2014, **2**, 5828–5836.
67 L. J. Zhu, L. P. Zhu, Y. F. Zhao, B. K. Zhu and Y. Y. Xu, *J. Mater. Chem. A*, 2014, **2**, 15566–15574.
68 K. Se, *Prog. Polym. Sci.*, 2003, **28**, 583–618.
69 A. B. Lowe and C. L. McCormick, *Prog. Polym. Sci.*, 2007, **32**, 283–351.
70 S. R. Williams and T. E. Long, *Prog. Polym. Sci.*, 2009, **34**, 762–782.
71 W. Jaeger, J. Bohrisch and A. Laschewsky, *Prog. Polym. Sci.*, 2010, **35**, 511–577.
72 D. D. Tang, X. Jiang, H. H. Liu, C. X. Li and Y. L. Zhao, *Polym. Chem.*, 2014, **5**, 4679–4692.
73 X. Jiang, W. Shao, K. Jiang, M. J. Zhang, H. H. Liu, C. N. Ye and Y. L. Zhao, *Polym. Chem*., 2013, **4**, 3272–3281.
74 M. J. Zhang, H. H. Liu, W. Shao, C. N. Ye and Y. L. Zhao, *Macromolecules,* 2012, **45**, 9312–9325.
75 Y. Mitsukami, M. S. Donovan, A. B. Lowe and C. L. McCormick, *Macromolecules*, 2001, **34**, 2248–2256.
76 W. Stöber, A. Fink and E. Bohn, *J. Colloid Interface Sci.*, 1968, **26**, 62–69.
77 N. Plumeré, A Ruff, B. Speiser, V. Feldmann and H. A. Mayer, *J. Colloid Interface Sci.*, 2012, **368**, 208–219.

This journal is © The Royal Society of Chemistry [year]